Analytical Methods

Accepted Manuscript

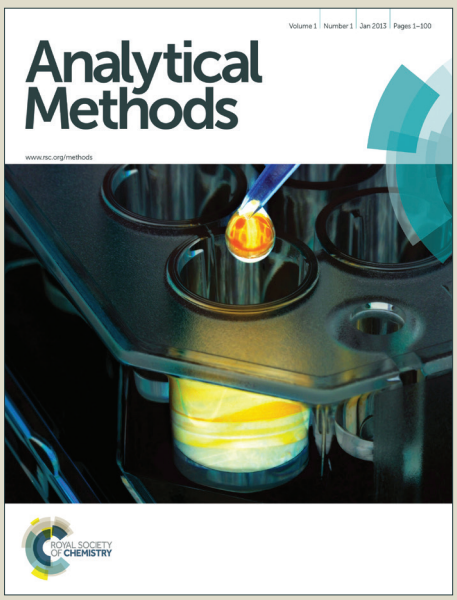

ROYAL SOCIETY OF CHEMISTRY

www.rsc.org/methods

Cite this: DOI: 10.1039/c0xx00000x

www.rsc.org/xxxxxx

PAPER

Glucoamylase-labeling nanogold flower for *in situ* enhanced sensitivity of glucometer-based enzyme immunoassay

Xiaohong Fu,* Kun Xu, Jun Ye, Jie Chen and Xueyu Feng

Received (in XXX, XXX) Xth XXXXXXXXX 200X, Accepted Xth XXXXXXXXX 200X

DOI: 10.1039/b000000x

Methods based on enzyme labels have been developed for glucometer-based immunoassays, but most involve low sensitivity and are unsuitable for routine use. Herein, we report a simple and sensitive enzyme immunoassay for the determination of neuron-specific enolase (NSE) by using glucoamylase-labeling nanogold flower (GA-NGF) for signal amplification. The assay is implemented in a polystyrene microtiter plate with a sandwich-type immunoassay format. In the presence of target analyte, the sandwiched immunocomplex can be formed in the microplate between capture antibody-functionalized microplate and detection antibody-conjugated GA-NGF. The carried glucoamylase accompanying nanogold flower can hydrolyze amylopectin in glucose, which can be quantitatively monitored by using a user-friendly personal glucometer (PGM). Under optimal conditions, the PGM signal increased with the increasing target NSE concentration in the dynamic working range of 0.01 – 30 ng mL^{-1} with a detection limit of 8 pg mL^{-1}. Importantly, the PGM-based immunoassay also displays good reproducibility, high specificity and comparable method accuracy with the referenced values.

Introduction

Recently, great effort has been expanded in the field of assay development, especially for immunoassay design, to simplify the assay procedure and cut down the assay cost while preserving the essential benefits in the sensitivity, robustness, broad applicability and suitability to automation.[1-3] One preferable approach is to utilize low-cost sensing transducers and user-friendly detection devices, particularly for developing countries.[4-6] The Tang group designed an integrated automatic electrochemical immunosensor array for simultaneous detection of five-type hepatitis virus antigens within 5 min by using a low-cost digital pH meter.[7] Parween and Nahar reported an image-based ELISA technique on an activated polypropylene microtest plate as an illustrative example of a spectrophotometer-free low cost diagnostic assay even in 8 min.[8] Wu et al. developed paper-based electrochemiluminescence origami cyto-device for multiple cancer cells detection using porous AuPd alloy as catalytically promoted nanolabels.[9] Despite many advances in this field, there is still the quest for more flexible, yet highly sensitive, quantitative, and easy-to-use methods to keep pace with expectations in future point-of-care testing.

Microtiter plate (MTP, as a low-cost small test device) has been become a standard tool in analytical research and clinical diagnostic testing laboratories.[10,11] Higgins et al. developed a high-throughput microplate assay for quantitation of neutral lipids in extracts from microalgae.[12] Sugi et al. utilized microplate assay for screening Toxoplasma godii bradyzoite differentiation with DUAL luciferase assay.[13] In this work, thus, we would like to utilize the low-cost microplate as the detection device for immunoassay development. Typically, the specific biological, chemical or physical events in samples stored in the microplate can be quantitatively monitored by microplate readers. In contrast, the emergence of portable personal glucometer opens a new horizon for the design of simplified detection devices.[14-16] Most recently, Tang et al. designed several advanced detection modes for the detection of adenosine triphosphate, biotoxin, heavy metal ion and aflatoxins with glucometer readout.[17-20] Favorably, our group also developed an enzyme immunoassay of quantitative determination of neuron-specific enolase in a high-binding polystyrene 96-well microplate by using a portable and user-friendly personal glucometer as the detection device.[21] Unfortunately, the detectable sensitivity was unreachable to the clinical threshold of many protein biomarkers because their concentrations in real-life biological samples are commonly down to pg mL^{-1} at the early stages of the diseases.

To achieve a high sensitivity for PGM-based immunoassay, enzyme label and nanolabel are usually used for this purpose.[21] Recently, we found that nanomaterials with different shapes exhibited various labeling abilities and analytical properties for the biomolecules, even at the same-component nanostructure. Rafique et al. investigated in detail the effects of three-type gold nanostructures including pyramid, spherical and rod-like nanostructures on the analytical performance of electrochemical immunoassay, and improved analytical properties could be achieved by using spherical gold nanostructures.[22] Lai et al. also monitored the effects of irregular-shaped gold nanoparticles and spherical gold nanoparticles on the sensitivity of electrochemical immunoassay.[23] Results indicated that use of irregular-shaped gold nanoparticles could exhibit higher voltammetric responses

than that of spherical gold nanoparticles. To this end, our motivation of this work is to synthesize nanogold flower (as the nanolablel) for the development of enzyme immunoassay.

For favorable comparison with our previous report based on spherical gold nanoparticle,[21] neuron-specific enolase (NSE) was also used as a model analyte for the construction of PGM-based enzyme immunoassay. Prior to experiment, monoclonal mouse anti-human NSE antibody-coated microplate and nanogold flower labeled with glucoamylase/polyclonal rabbit anti-human NSE antibody were used as the capture antibody and detection antibody, respectively. In the presence of target analyte, a sandwiched immunocomplex could be formed between capture antibody and detection antibody in the microplate. Upon addition of amylopectin introduction in the microplate, the glucoamylase could hydrolyze it into numerous glucose molecules, which could be monitored by using a portable glucometer. The readable signal indirectly increased with the increasing NES concentration. The aim of this study is to exploit a highly sensitive immunoassay for the detection of low-abundant protein in biological fluids.

Experimental

Materials and reagent

High-binding polystyrene 96-well microplate (Greiner Bio-one, Frickenhausen, Germany) and personal glucometer (PGM, Roche, Accu-Chem® Active, Malaysia) were used in all runs. Mouse anti-human monoclonal NSE (mAb_1), rabbit anti-human polyclonal NSE (pAb_2) and NSE standards were achieved from Biosynth. Biotech. CO., Ltd. (Beijing, China). Glucoamylase (140 000 units mL^{-1}), amylopectin from potato starch and bovine serum albumin (BSA) were purchased from Sigma-Aldrich (USA). PGM buffer (pH 7.3, 72.9 mM Na_2HPO_4 + 27.1 mM NaH_2PO_4 + 50 mM NaCl + 5 mM $MgCl_2$) was prepared by adding the chemicals into 1000 mL distilled water. The washing buffer was achieved by throwing 0.05% Tween 20 (v/v) (Genview, USA) in PGM buffer. Other reagents were of analytical grade. Ultrapure water based on Millipore purification system (18.2 MΩ cm^{-2}, Milli-Q, Millipore) was used in all runs.

Synthesis of nanogold flower (NGF)

Nanogold flower with an average size of 50 nm in diameter along its horizontal or longitudinal axis was synthesized according to the literature with minor revision.[24] Initially, 1 mL of 0.02 M ascorbic acid was added to 10 mL of chitosan acetic acid solution (5 mg mL^{-1}), and the mixture was diluted to 24-mL distilled water. After adequately stirring, 1.25-mL $HAuCl_4$ (2.5 wt ‰) aqueous solution was quickly injected to the resulting mixture. Following that, the suspension (dark blue) was centrifuged for 10 min at 8000 g. The obtained pellets (*i.e.* nanogold flower, designated as NGF) were dispersed into 5-mL distilled water, and stored in a dark colored bottle at 4 °C for further usage.

Labeling of NGF with glucoamylase and detection antibody

Glucoamylase and detection antibody were labeled to nanogold flower referring to our previous report.[21] Before the conjugation, nanogold flower colloids prepared above were adjusted to pH 9.0 using Na_2CO_3. Following that, a 200-μL mixture containing 150-μL glucoamylase (140 000 units mL^{-1}) and 50-μL pAb_2 detection antibody (1.0 mg mL^{-1}) were injected to the suspension, and reacted for 6 h at 4 °C with gentle shaking. Afterwards, the suspension was centrifuged for 15 min (8000 g) at 4 °C. Finally, the obtained pellets (*i.e.* NGF-labeled glucoamylase and detection antibody, designated as GA-NGF-pAb_2) were dispersed into 1-mL pH 7.3 PGM buffer.

Monitoring of target NSE with glucometer readout

Before measurement, monoclonal anti-NSE capture antibody-coated microplate (mAb_1-MTP) was prepared, and the process was described in detail in our previous report.[21] The PGM assay was carried out as follows: (i) 50-μL NSE sample was added to the mAb_1-MTP and reacted for 25 min at 37 °C under gentle shaking, (ii) 50-μL GA-NGF-pAb_2 prepared above was injected into the resulting mAb_1-MTP and reacted for 25 min under the same condition, (iii) 20-μL amylopectin (0.5 mg mL^{-1}) in pH 7.3 PGM buffer was added to the microplate and hydrolyzed for 35 min 50 ºC, and (iv) a 3-μL aliquot of the supernatant was dropped onto the PGM for glucose measurement. The obtained PGM signal was registered as the sensing signal relative to different-concentration target NSE. After each step, the microplate was washed by using the washing buffer.

Results and discussion

Design of PGM-based enzyme immunoassay

Scheme 1 gives the assay procedure and basic mechanism of the PGM-based immunosensing protocol in the functional microplate by using GA-NGF-pAb_2 as the signal-transduction tag with glucometer readout. Monoclonal anti-human NSE antibody was physically adsorbed to the microplate through the interaction between protein and high-binding polystyrene microplate.[25-27] Nanogold flower was synthesized by the reduction of $HAuCl_4$ in the presence of chitosan. Glucoamylase and antibody were conjugated onto the NGF surface through the interaction between cystein or NH_3^+-lysine residues of protein and nanogold flower.[28] Use of nanogold flower was expected to enhance the surface coverage of nanostructure for the conjugation of biomolecules. In the presence of target NSE, the as-prepared GA-NGF-pAb_2 was assembled to the mAb_1-MTP through the antigen-antibody reaction. The conjugation amount of GA-NGF-pAb_2 in the microplate increased with the increasing NSE concentration in the sample. Upon amylopectin introduction, the glucoamylase accompanying GA-NGF-pAb_2 could hydrolyze the amylopectin into many glucose molecules. The produced glucose could be quantitatively determined by using a user-friendly personal glucometer. By evaluating the change in the PGM signal, we could indirectly calculate the concentration of NSE in the detection solution.

Fig. 1A shows typical transmission electron microscope (TEM) of the as-prepared nanogold flower. A flower-like structure was obviously observed with an average size of 50 nm. Such a structure could provide a large room for the labeling of biomolecules. To realize our design, one important precondition for the successful development of PGM-based immunoassay is whether the glucoamylase could be readily conjugated to nanogold flower by our designed route. To demonstrate this point, the as-prepared GA-NGF-pAb_2 was directly used for the reaction with amylopectin solution. Meanwhile, the amylopectin solution was determined by using a portable PGM before and after reaction with GA-NGF-pAb_2. As seen from curve '*a*' in Fig. 1B,

the PGM signals were not almost changed over 60 min, indicating that the amylopectin could not produce the PGM signal. When glucoamylase was added into the amylopectin, however, the PGM signal increased with the increasing reaction time, and tended to level off after 35 min. The results revealed that introduction of GA-NGF-pAb_2 could cause the production of glucose molecules. Logically, another question arises to be answered whether the PGM signal derived from nanogold flower or pAb_2. As control test, we also synthesized pAb_2-labeled NGF (NGF-pAb_2) using the similar method, which was investigated by using mentioned-above method. Experimental results indicated that the NGF-pAb_2 could not hydrolyze the added amylopectin (data not shown). Thus, we might make a conclusion that (i) glucoamylase could be labeled to nanogold flower, and (ii) the labeled glucoamylase on the NGF could hydrolyze the amylopectin into glucose, not deriving from nanogold flower and pAb_2 antibody.

Further, we also investigated whether the PGM signal really originated from target-induced assembly of GA-NGF-pAb_2 during the measurement. To verify this concern, the as-prepared mAb_1-MTP and GA-NGF-pAb_2 were utilized for the detection of zero analyte and 1.0 ng mL^{-1} NSE, respectively. Following that, the PGM signal was collected and recorded intermittently (every 5 minutes) after addition of amylopectin into the resulting microplate (Fig. 1C). As seen from curve '*a*', the PGM signal was almost unchanged over 50 min in the absence of target NSE, indicating that the added amylopectin was not hydrolyzed into glucose. In the presence of target NSE, however, the PGM signal increased with the increasing reaction time, and reached the steady-state signal after ~35 min (curve '*b*'). The results also revealed that (i) target NSE could trigger the assembly of GA-NGF-pAb_2, thereby resulting in the progression of hydrolysis reaction; and (ii) it took some time (~35 min) for the hydrolysis reaction through the labeled glucoamylase on the GA-NGF-pAb_2 toward the enzymatic substrate, amylopectin. To avoid possible error resulting from different-batch samples, all PGM signals obtained in this work were collected and registered at 35 min after addition of target analyte. The results further revealed that the GA-NGF-pAb_2 could not be non-specifically adsorbed to the mAb_1-MTP. Therefore, our design could be preliminarily applied for the monitoring of target analyte by using GA-NGF-pAb_2 as the signal-transduction tag accompanying glucometer readout.

Optimization of experimental conditions

In this work, the detectable PGM signal mainly derives from the labeled glucoamylase on nanogold flower toward the hydrolysis of the amylopectin. Since the glucoamylase and pAb_2 antibody were co-immobilized on nanogold flower, the conjugation ratio of glucoamylase and pAb_2 should be one of the most important factors influencing the sensitivity of PGM-based immunoassay. Usually, highly carried amount of pAb_2 antibody on the NGF could increase the possiblity of the antigen-antibody reaction, but it is not conducive to the hydrolysis reaction, thus resulting in a weak PGM signal. As indicated from Fig. 2A, the maximum PGM signal could be achieved at the volume ratio of 3 : 1. So, 150-μL glucoamylase (140 000 units mL^{-1}) and 50-μL pAb_2 detection antibody (1.0 mg mL^{-1}) was used for the preparation of GA-NGF-pAb_2.

Usually, the antigen-antibody reaction is carried out at human normal body temperature (37 °C). At this condition, we monitored the effect of incubation time on the signal of PGM-based enzyme immunoassay from 10 min to 35 min (*Note*: To avoid confusion, the incubation time of mAb_1-MTP with NSE was paralleled with that of the MTP-mAb_1-CEA with GA-NGF-pAb_2). As shown in Fig. 2B, the PGM signal increased with the increment of incubation time, and tended to level off after 25 min. Hence, an incubation time of 25 min was selected for sensitive determination of NSE in this work.

Another important issue for the detectable PGM signal was the hydrolysis time of glucoamylase toward the amylopectin. Usually, it takes some time for the bioactive enzyme to catalyze enzymatic substrate. As seen from Fig. 2C, a relatively strong PGM signal could be recorded after 35 min, indicating that the hydrolysis reaction of glucoamylase tended to the equilibrium. So, 35 min was chosen for enzymatic hydrolysis reaction.

Dose response of PGM-based enzyme immunoassay

To quantitatively monitor target analyte, different-concentration NSE standards were measured in the mAb_1-MTP by using the as-prepared GA-NGF-pAb_2 as the signal-transduction tag with the glucometer readout. As shown from Fig. 3A, we could clearly observe that with the increasing NSE concentration in the sample the digital signal of the glucometer increased accordingly in the range of 0 to 50 ng mL^{-1} and almost tended to level off thereafter. Under optimal conditions, a good linear relationship [PGM signal (mM) *vs*. NSE concentration (ng mL^{-1})] in the dynamic working range of 10 pg mL^{-1} to 30 ng mL^{-1} was obtained, and as low as 8 pg mL^{-1} NSE could be unambiguously monitored. The linear regression equation was y (mM) = 0.9028 × $C_{[NSE]}$ + 0.1202 (ng mL^{-1}, R^2 = 0.9935, n = 18). Obviously, the detection limit (LOD) of the developed enzyme immunoassay was lower than that of our previous report[21] (using spherical gold nanoparticle as the signal-transduction tag, LOD: 50 pg mL^{-1}). Moreover, the slope (0.9028) of the linear regression equation was higher than that of previous work (0.5044). To further elucidate the advantage of using nanogold flower as the signal-transduction tag, the LOD was compared with existed NSE ELISA kits from different companies (CusaBio Biotech. Inc.: 390 pg mL^{-1}, MyBioSource, Inc.: 390 pg mL^{-1}, Wuhan EIAab Sci. Inc.: 156 pg mL^{-1}, Diagnostic Automation Inc.: 15 ng mL^{-1}, USCN Life Sci. Inc.: 7.2 pg mL^{-1}, Alpha Diagnostic Intl.: 1.0 ng mL^{-1}). Such a low detection limit was possibly due to the signal amplification by the massive glucoamylase on nanogold flower and the inherent high enzymatic turnover of glucoamylase.

Specific, precision and reproducibility

The reproducibility and precision of the as-prepared mAb_1-MTP and GA-NGF-pAb_2 for the determination of target NSE were investigated (1.0 ng mL^{-1} NSE used in this case). As shown from Fig. 3B, the relative standard deviation (RSD, n = 7) was ~9.2% for the same-batch mAb_1-MTP and GA-NGF-pAb_2, while that was ~12.1% (n = 7) with different batches. For comparison, we calculated the RSD (RSD = 10.8%) during the 12 assays. Thus, the reproducibility and precision of the PGM-based enzyme immunoassay was acceptable.

Further, we evaluated the selectivity and specificity of PGM-based enzyme immunoassay by challenging other low-abundant proteins, *e.g.* myc-oncogene (MYC, 50 ng mL^{-1}), squamous cell carcinoma antigen (SCCA, 50 ng mL^{-1}), alpha-fetoprotein (AFP, 50 ng mL^{-1}), and thyroid-stimulating hormone (TSH, 50 ng mL^{-1}). As seen from Fig. 4A, all the interfering materials did not cause the significant increase in the PGM signal relative to the control test, regardless of detection alone or mixture assay. The

high specificity was ascribed to the specific antigen-antibody reaction.

Monitoring of real samples

To elucidate the analytical reliability and applicable potential of the PGM-based enzyme immunoassay, three NSE human serum specimens were collected from the local Second People's Hospital (Chengdu, China). Each specimen was initially diluted to various samples (n = 5) with new-born cattle serum. Then, 15 samples were determined by using PGM-based enzyme immunoassay. The obtained results were compared with the reference values obtained by Electrochemiluminescent (ECL) Automatic Analyzer (provided by hospital) (Fig. 4B). As shown from Fig. 4B, the slope and intercept of the regression equation between two methods were close to ideal '1' and '0', respectively, toward all the serum samples, indicating a good correlation between the PGM-based enzyme immunoassay and referenced ECL immunoassay. The results further revealed that the as-prepared mAb_1-MTP and GA-NGF-pAb_2 could be preliminarily employed for quantitative monitoring of target NSE in real sample by coupling with a portable personal glucometer.

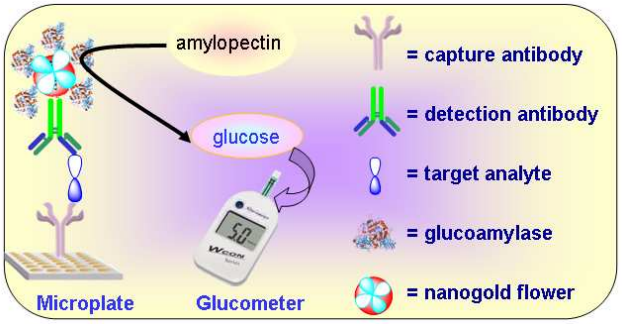

Scheme 1 Schematic illustration of PGM-based enzyme immunoassay in capture antibody-coated microtiter plate by using glucoamylase and detection antibody-conjugated nanogold flower as the signal-transduction tag with glucometer readout.

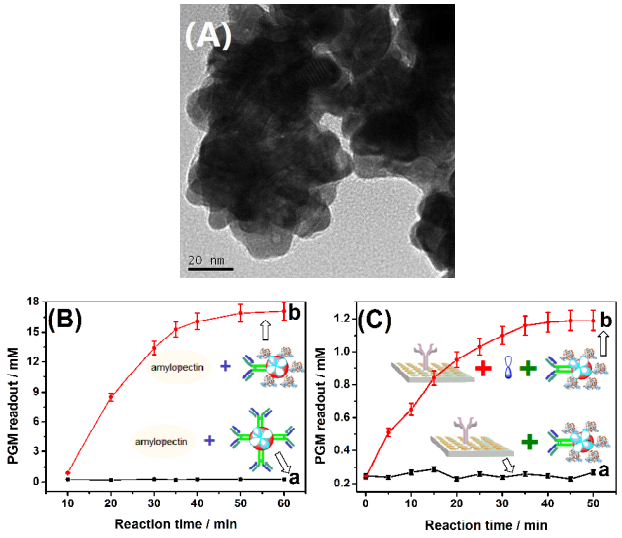

Fig. 1 (A) Typical TEM image of the as-synthesized nanogold flowers, (B) PGM readout (versus reaction time) of (a) pAb$_2$-NGF + amylopectin and (b) GA-NGF-pAb$_2$ + amylopectin, and (C) PGM readout (versus reaction time) of (a) mAb$_1$-MTP + GA-NGF-pAb$_2$ and (b) mAb$_1$-MTP + 1.0 ng mL^{-1} NSE + GA-NGF-pAb$_2$.

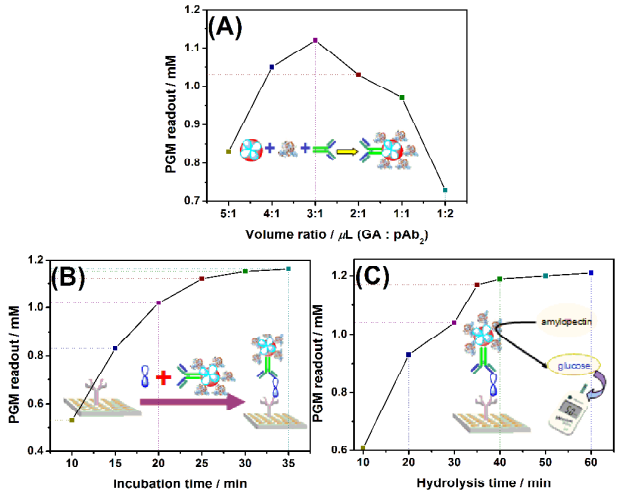

Fig. 2 The effects of (A) volume ratio between glucoamylase (140 000 units mL^{-1}) and pAb$_2$ (1.0 mg mL^{-1}) for the preparation of GA-NGF-pAb$_2$, (B) incubation time for the antigen-antibody reaction, and (C) hydrolysis time of the labeled glucoamylase on GA-NGF-pAb$_2$ toward amylopectin on the readout signal of PGM-based enzyme immunoassay (1.0 ng mL^{-1} NSE used in this case) .

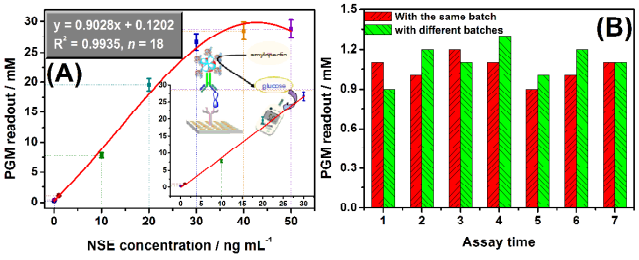

Fig. 3 (A) Readout signals of PGM-based enzyme immunoassay toward NSE standards with different concentration in mAb$_1$-MTP by using GA-NGF-pAb$_2$ as the signal-transduction tag (inset: calibration curve), and (B) the precision and reproducibility of PGM-based enzyme immunoassay by using the same-batch mAb$_1$-MTP/GA-NGF-pAb$_2$ and different-batch mAb$_1$-MTP/GA-NGF-pAb$_2$, respectively (1.0 ng mL^{-1} NSE used in this case).

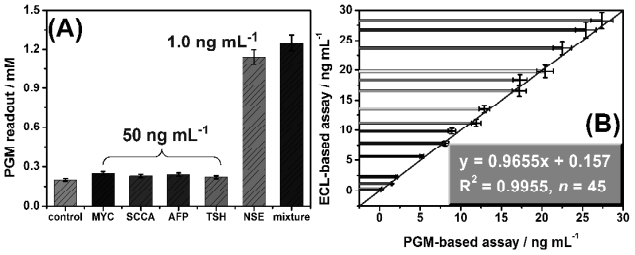

Fig. 4 (A) The specificity of PGM-based enzyme immunoassay against MYC, SCCA, AFP, TSH and target NSE (note: The mixture contained

50 ng mL^{-1} MYC, 50 ng mL^{-1} SCCA, 50 ng mL^{-1} AFP, 50 ng mL^{-1} TSH and 1.0 ng mL^{-1} NSE), and (B) comparison of the assayed results for human serum specimens by using PGM-based enzyme immunoassay and referenced ECL immunoassay (note: Each data represents the average value of three measurements, whereas the real level of NSE in the specimens was evaluated according to the mentioned-above regression equation, $y = 0.9028 \times C_{[NSE]} + 0.1202$).

Conclusions

In summary, we demonstrate the development of an advance enzyme immunoassay in a low-cost microplate by using personal glucometer as the detection device. Use of nanogold flowers (as the signal-transduction tag) improved the analytical properties of PGM-based enzyme immunoassay, and enhanced the sensitivity in comparison with our previous report[21] (using spherical gold nanoparticle as the signal-transduction tag). Moreover, the results assayed toward clinical serum samples were comparable with those by commercialized available ECL-based immunoassay. Importantly, the PGM-based sensing platform can be widely used in developing countries without the requirement of sophisticated equipment. To fully assess the application potential and the added value of PGM-based enzyme immunoassay, future works should focus on other low-abundant proteins and sample types.

Support by the Scientific Research Fund of Sichuan Provincial Education Department (grant no. 14ZA0303), the Natural Science Foundation of Sichuan Province (grant nos. 2014JY0117 & 2013sz0054), and the Key Project of Chengdu Normal University (grant no. CS13ZA02) is gratefully acknowledged.

Notes and references

Department of Chemistry and Bioscience, Chengdu Normal University, Chengdu 611130, P.R. China. E-mail: xiaohong.fuzq@gmail.com; Fax: +86 28 6677 2014; Tel: +86 28 6677 2040

1 H. Akhavan-Tafti, D. Binger, J. Blackwood, Y. Chen, R. Creager, R. de Silva, R. Eickholt, J. Gaibor, R. Handley, K. Kapsner, S. Lopac, M. Mazelis, T. McLernon, J. Mendoza, B. Odegaard, S. Reddy, M. Salvati, B. Scchoenfelner, N. Shapir, K. Shelly, J. Todtleben, G. Wang and W. Xie, *J. Am. Chem. Soc*., 2013, **135**, 4191-4194.
2 X. Fu, R. Huang, J. Wang and X. Feng, *Anal. Methods*, 2013, **5**, 3803-3806.
3 S. Lee, G. Park, S. Chakkarapani and S. Kang, *Biosens. Bioelectron*., 2015, **63**, 444-449.
4 X. Fu, R. Huang, J. Wang and B. Cheng, *RSC Adv.,* 2013, **3**, 13451-13456.
5 J. Hu, T. Wang, J. Kim, C. Shannon and C. Easley, *J. Am. Chem. Soc*., 2012, **134**, 7066-7072.
6 B. Zhang, B. Liu, G. Chen and D. Tang, *Biosens. Bioelectron*., 2015, **64**, 6-12.
7 D. Tang, J. Tang, B. Su, J. Ren and G. Chen, *Biosens. Bioelectron*., 2010, **25**, 1658-1662.
8 S. Parween and P. Nahar, *Biosens. Bioelectron*., 2013, **48**, 287-292.
9 L. Wu, C. Ma, L. Ge, Q. Kong, M. Yan, S. Ge and J. Yu, *Biosens. Bioelectron*., 2015, **63**, 450-457.
10 B. Cheong, W. Chua, O. Liew and T. Ng, *Anal. Biochem*., 2014, **458**, 40-42.
11 Q. Lang, F. Wang, L. Yin, M. Liu, V. Petrenko and A. Liu, *Anal. Chem*., 2014, *86*, 2767-2774.
12 B. Higgins, A. Thornton-Dunwoody, J. Labavitch and J. Vandergheynst, *Anal. Biochem.*, 2014, **465**, 81-89.
13 T. Sugi, T. Masatani, F. Murakoshi, S. Kawaze and K. Kato, *Anal. Biochem*., 2014, **464**, 9-11.
14 Q. Wang, F. Liu, X. Yang, K. Wang, H. Wang and X. Deng, *Biosens. Bioelectron*., 2015, **64**, 161-164.
15 J. Chen, W. Wu and L. Zeng, *Anal. Methods*, 2014, *6*, 4840-4844.
16 K. Cha, G. Jensen, A. Balijepalli, B. Cohan and M. Meyerhoff, *Anal. Chem*., 2014, **86**, 1902-1908.
17 D. Tang, Y. Lin, Q. Zhou, Y. Lin, P. Li, R. Niessner and D. Knopp, *Anal. Chem*., 2014, doi:10.1021/ac503616d.
18 L. Hou, C. Zhu, X. Wu, G. Chen and D. Tang, *Chem. Commun.*, 2014, **50**, 1441-1443.
19 Z. Gao, D. Tang, M. Xu, G. Chen and H. Yang, *Chem. Commun*., 2014, **50**, 6256-6258.
20 L. Fu, J. Zhuang, W. Lai, X. Que, M. Lu and D. Tang, *J. Mater. Chem. B*, 2013, **1**, 6123-6128.
21 X. Fu, X. Feng, K. Xu and R. Huang, *Anal. Methods*, 2014, **6**, 2233-2238.
22 S. Rafique, C. Gao, C. Li and A. Bhatti, *J. Appl. Phys*., 2013, **114**, art. 164703.
23 W. Lai, D. Tang, X. Que, J. Zhuang, L. Fu and G. Chen, *Anal. Chim. Acta*, 2012, **755**, 62-68.
24 W. Wang, X. Yang and H. Cui, *J. Phys. Chem. C*, 2008, **112**, 16348-16353.
25 A. Saini, J. Kumar and J. Melo, *Anal. Chim. Acta*, 2014, **849**, 50-56.
26 S. Vermeir, B. Nicolai, P. Verboven, P. Van Gerwen, B. Baeten, L. Hoflack, V. Vulsteke and J. Lammertyn, *Anal. Chem.*, 2007, **79**. 6119-6127.
27 F. Robert-Peillard, J. Boudenne and B. Coulomb, *Food Chem*., 2014, **150**, 274-279.
28 D. Tang, B. Zhang, J. Tang, L. Hou and G. Chen, *Anal. Chem*., 2013, **85**, 6958-6966.

For Only Graphic Abstract